

Transport in a Modulated One-Dimensional Ballistic Channel

C.-T. Liang^{1,2}, M. Pepper², M. Y. Simmons^{2,3}, C. G. Smith², Gil-Ho Kim^{2,4} and D. A. Ritchie²

¹*Department of Physics, National Taiwan University, Taipei, Taiwan 106, R.O.C.*

²*Cavendish Laboratory, Madingley Road, Cambridge CB3 0HE, United Kingdom*

³*School of Physics, University of New South Wales, Sydney 2052, Australia*

⁴*Telecommunication Basic Research Laboratory, ETRI, Yusong P. O. Box 106, Daejeon 305-600, Korea*

(Received August 21, 2001)

In this paper we review measurements on a modulated one-dimensional (1D) ballistic channel. We have designed a novel 1D channel with three separate and independently contacted overlaying finger gates. By changing the applied voltages on the overlaying gate fingers, we are able to vary the potential modulation in a ballistic 1D channel. Our experimental results fall into two categories. (i) We show that “the 0.7 structure” [K. J. Thomas *et al.*, Phys. Rev. Lett. 77, 135 (1996)] persists despite a change of the lateral confinement strength by a factor of 2. We have also shown that the 0.7 structure present in two 1D channels in series behaves like a single 1D channel, demonstrating that the 0.7 structure is not a transmission effect through a ballistic channel at zero in-plane magnetic field. (ii) In our versatile system, an open quantum dot can be electrostatically defined by a split-gate, and two overlaying finger gates which introduce entrance and exit barriers to the dot. In this case, we observe continuous and periodic oscillations superimposed upon ballistic conductance steps at zero magnetic field. We ascribe the observed conductance oscillations, when the conductance through the dot G exceeds $2e^2/h$, to experimental evidence for Coulomb charging effects in an open dot [C.-T. Liang *et al.*, Phys. Rev. Lett. 81, 3507 (1998)]. This is supported by the evolution of the oscillatory features for $G > 2e^2/h$ as a function of both temperature and barrier transparency. Moreover, we present clear experimental evidence that coherent resonant transport and Coulomb charging effects co-exist in our system.

PACS. 73.20.Dx – Electron states in low-dimensional structures.

PACS. 73.40.Gk – Tunneling.

I. Introduction

Using the now well-established “split-gate” technique [1], it is possible to define a one-dimensional (1D) channel within a two-dimensional electron gas (2DEG). If the elastic scattering length is longer than the 1D channel length, one may observe ballistic conductance plateaux quantised in units of $2e^2/h$ [2, 3] at zero magnetic field, with the factor of 2 from the electron spin degeneracy. When a large in-plane magnetic field is applied parallel to the 1D channel, such that the electron spin degeneracy is lifted, conductance plateaux quantised in units of e^2/h are observed [4]. Quantised conductance plateaux in units of $2e^2/h$ at zero magnetic field (e^2/h at high parallel fields) observed in a 1D channel can be well explained by cancellation of the Fermi velocity and 1D density of states within a single-particle picture.

In very clean 1D channels a clear plateau-like structure close to $(0.7 \times 2e^2/h)$ has been observed at zero magnetic field $B = 0$ [5]. This “0.7 structure” whose conductance value is placed between the spin-degenerate conductance plateau at $2e^2/h$ and the spin-split conductance plateau at e^2/h , cannot be explained within a single-particle picture. The fact that the 0.7 structure evolves into a $(0.5 \times 2e^2/h)$ spin-split conductance plateau on the application of an in-plane magnetic field suggests the structure is spin related. The 0.7 structure has also been observed in 1D channels with many different sample designs [5-14], establishing that it is a universal effect. In particular, Kristensen *et al.* [8, 12] reported activated behaviour of the 0.7 structure as a function of temperature with a density-dependent activation temperature of around 2 K. Various theoretical models [15-20] have been proposed to explain the undisputed “0.7 structure”, however, its exact physical origin remains unknown.

Electrostatically-shaped semiconductor quantum dots with discrete zero-dimensional (0D) electronic states [21] have been attracting a great deal of theoretical and experimental interest. Consider a lateral quantum dot weakly coupled to the source and drain contacts where the tunnelling conductance through the dot G is low, $G \ll 2e^2/h$. If the thermal smearing $k_B T$ and the chemical potentials in the leads are much smaller than the Coulomb charging energy e^2/C , which is required for adding an extra electron to the quantum dot, transport through the dot is inhibited. This is the Coulomb blockade (CB) of single electron tunnelling [22, 23]. It has been demonstrated [24] that transport through a small quantum dot is determined by Coulomb charging effects [25] (quantisation of charge) as well as quantum confinement effects [26, 27] (quantisation of energy). At present, it is widely accepted that, at zero magnetic field, the conductance $2e^2/h$ is the upper limit for which Coulomb charging effects can occur [28]. Nevertheless, there is experimental evidence [29-31] which appears to contradict this concept.

In this paper, we review measurements on clean modulated 1D ballistic channels [32-34]. We have designed a novel 1D channel with three separate and independently contacted overlaying finger gates. Our device can be operated in two regimes. First, by biasing a single overlaying finger gate, we are able to vary both the lateral confinement strength and the potential profile within the 1D channel. In this regime, we find that the 0.7 structure is an intrinsic property of a clean 1D channel well over the range investigated. Moreover, we shall present clear experimental evidence that the 0.7 structure is not a transmission effect at zero in-plane magnetic field. Second, in our system we can also have a strongly modulated 1D channel with double barriers. In this case, we observe continuous and periodic oscillations superimposed upon ballistic conductance steps at zero magnetic field. The observed conductance oscillations, when the conductance through the dot G exceeds $2e^2/h$, are ascribed to experimental evidence for Coulomb charging effects in an open quantum dot. The rest of this paper is organised as follows. Section II describes transport in a modulated 1D channel in which we investigate the “0.7 structure”. Section III presents measurements on a strongly modulated 1D channel with double barriers in which we observe evidence for Coulomb charging effects in an open quantum dot device when G is greater than $2e^2/h$. In Section IV we summarise our experimental results, together with some conclusions.

II. Measurements on a modulated 1D channel

Figure 1(a) shows a schematic diagram of the device configuration. The device was defined by electron beam lithography, 157 nm above the 2DEG. There is a 30 nm-thick layer of polymethylmethacrylate (PMMA) which has been highly dosed by an electron beam, to act as a

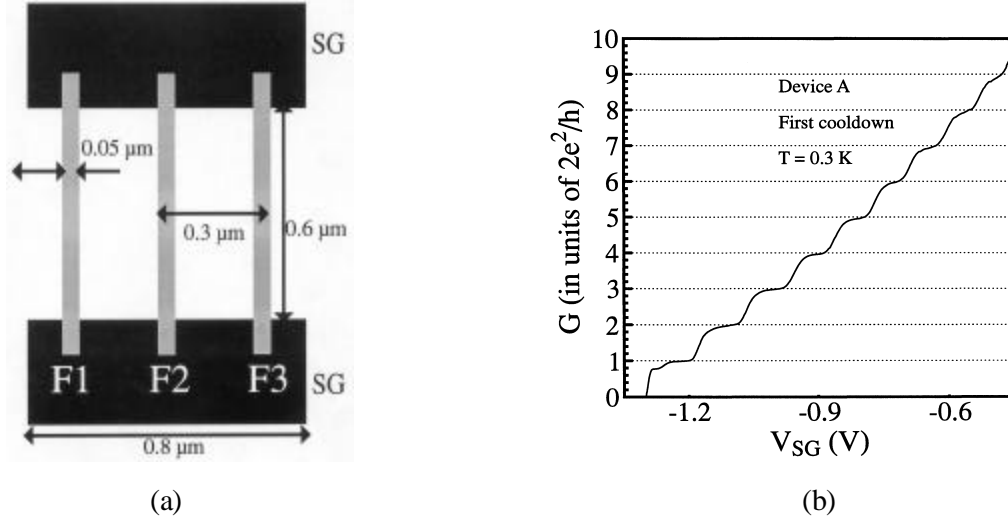


FIG. 1. (a) Schematic diagram showing the device configuration. The grey regions correspond to finger gates, labelled as F1, F2, and F3 lying above the split-gate (labelled as SG), with an insulating layer of crosslinked PMMA in between. (b) $G(V_{SG})$ for all finger gates at 0 V. The measurement temperature was 300 mK.

dielectric [35] between the split-gate (SG) and three gate fingers (F1, F2 and F3) so that all gates can be independently controlled. The carrier concentration of the 2DEG was $1.9 \times 10^{15} \text{ m}^{-2}$ with a mobility of $250 \text{ m}^2/\text{Vs}$ after brief illumination with a red light emitting diode. The transport mean free path is 16.5 nm , much longer than the effective 1D channel length. The two-terminal conductance $G = dI/dV$ was measured using an ac excitation voltage of 10 mV with standard phase-sensitive techniques. In all cases, a zero-split-gate-voltage series resistance ($\approx 900 \text{ } \Omega$) is subtracted from the raw data. The in-plane magnetic field B_{\parallel} is applied parallel to the source-drain current. Four samples on six different runs showed similar behaviour, and the data that we present here are obtained from three devices A, B and C.

To demonstrate the high-quality of our 1D channel, figure 1(b) shows the conductance measurements $G(V_{SG})$ as a function of split-gate voltage V_{SG} when all finger gate voltages V_{F1} , V_{F2} and V_{F3} are zero at $T = 300 \text{ mK}$. We observe conductance plateaux at multiples of $2e^2/h$, with no resonant feature superimposed on top, demonstrating that we have a clean 1D channel in our system in which impurity scattering is negligible. In addition, we also observe the 0.7 structure.

We now describe the effects of applying a negative finger gate voltage V_{F2} . Figure 2(a) shows $G(V_{SG})$ for various voltages on F2 while F1 and F3 are at 0 V. The results presented here are taken at a measurement temperature of 1.2 K, since the 0.7 structure is known to be more pronounced at higher temperatures [5]. Increasing the negative voltage on F2 decreases the electron density underneath the finger gate. We use a technique developed by Patel *et al.* [36] to measure the energy separation of the 1D subbands from the effects of an applied dc source-drain voltage V_{sd} at various V_{F2} . The results are presented in Fig. 2(b); they have a good linear fit $\epsilon_{E_{1;2}} = (0.915 V_{F2}/V + 2.71) \text{ (meV)}$. It can be seen that as V_{F2} is made more negative, the

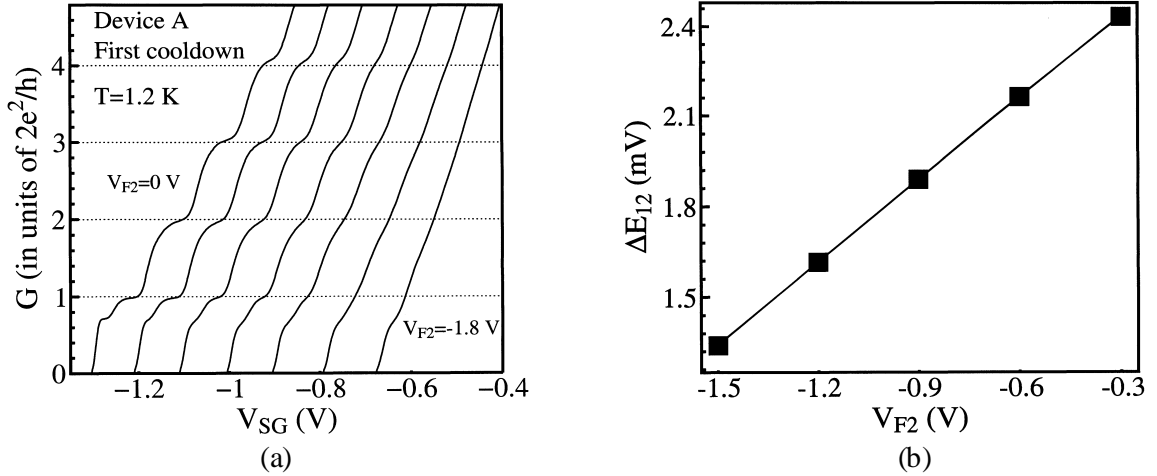


FIG. 2. (a) $G(V_{SG})$ for $V_{F2} = 0$ to ± 1.8 V in 0.3 V steps when $V_{F1} = V_{F3} = 0$ V. The measurement temperature was 1.2 K. (b) $\Delta E_{1,2}(V_{F2})$ (marked by squares) determined by the source-drain bias technique. The linear fit is discussed in the text.

energy spacing $\Delta E_{1,2}(V_{F2})$ decreases, giving rise to the reduction in flatness of the conductance plateaus presented in Fig. 2(a). Using the saddle point model [37], we estimate that the value $\Delta E_{1,2}$ decreases from 1.1 to 0.6 over the measurement range -0.3 V $\leq V_{F2} \leq 1.8$ V. Whilst the 1D ballistic conductance plateaus are no longer observable, the shoulder-like structure close to $G = (0.7 \pm 2e^2/h)$ is observed to persist despite this change in the lateral confinement strength. The data shown in figure 2(a) provide compelling evidence that the 0.7 structure is intrinsic to a clean 1D channel and persists over a wide range of lateral confinement strengths.

To demonstrate that the observed shoulder-like structure close to $0.7 \pm 2e^2/h$, where the conductance steps are not well-quantised and pronounced, has the same physical origin as those which coexist with well-quantised conductance steps [5], we have measured $G(V_{SG})$ at various B_k . As the applied B_k is increased, the shoulder-like feature indeed evolves into a spin-split ($0.5 \pm 2e^2/h$) conductance plateau, as clearly shown in figure 3, in agreement with the early studies of Thomas *et al.* [5]. The fact that the structure at $(0.7 \pm 2e^2/h)$ is not replicated at $0.7 \pm e^2/h$ when the spin degeneracy is removed at high B_k supports previous results by Thomas *et al.* [5].

We now present clear experimental evidence that the 0.7 structure is not a transmission effect at zero in-plane magnetic field. The solid line in figure 4 shows $G(V_{SG})$ when $V_{F1} = \pm 0.22$ V, $V_{F2} = 0$ V and $V_{F3} = 0$, and the dotted line shows $G(V_{SG})$ when $V_{F1} = 0$ V, $V_{F2} = 0$ V and $V_{F3} = \pm 0.3$ V. In both cases, we observe the 0.7 structure at the same V_{SG} so that the two barriers underneath the gate fingers are of the same heights. If we now set $V_{F1} = \pm 0.22$ V, $V_{F2} = 0$ and $V_{F3} = \pm 0.3$ V, we obtain the dashed line in figure 4. From the data for $V_{F1} = V_{F2} = V_{F3} = 0$, we know that for $V_{SG} = \pm 2.67$ V there are two 1D subbands present in the ballistic channel defined by SG. As illustrated in Fig. 4, the 1D channel pinches off at $V_{SG} = \pm 2.67$ V for both cases when $V_{F1} = \pm 0.22$ V and $V_{F3} = 0$, and $V_{F1} = 0$ and $V_{F3} = \pm 0.3$ V. The distance between F1 and F3 is twice as much as the distance between F1 (F3) and the underlying 2DEG. Also the

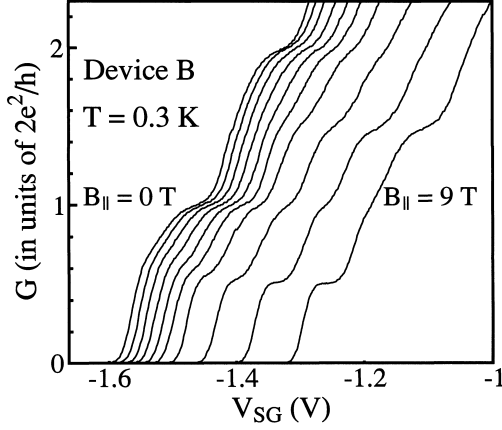


FIG. 3. $G(V_{SG})$ at various applied in-plane magnetic fields B_k for $V_{F2} = \pm 1.4$ V and $V_{F1} = V_{F3} = 0$ V. From left to right: $B_k = 0$ to 9 T in 1 T steps. Successive traces have been horizontally offset by 3 mV for clarity. The measurement temperature was 300 mK.

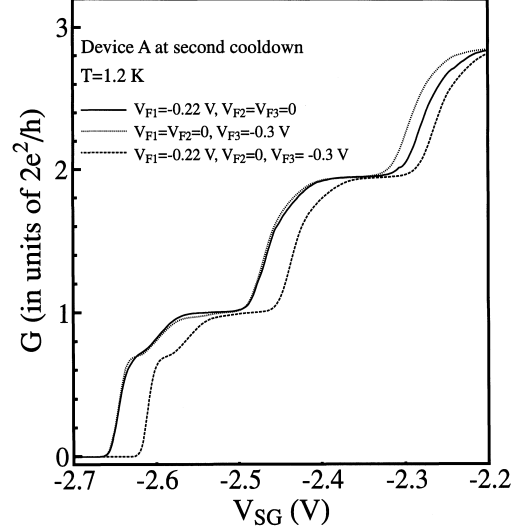


FIG. 4. The solid line shows $G(V_{SG})$ when $V_{F1} = \pm 0.22$ V, $V_{F2} = 0$ V and $V_{F3} = 0$, and the dotted line shows $G(V_{SG})$ when $V_{F1} = 0$ V, $V_{F2} = 0$ and $V_{F3} = \pm 0.3$ V. The dashed line shows $G(V_{SG})$ when $V_{F1} = \pm 0.22$ V, $V_{F2} = 0$ V and $V_{F3} = \pm 0.3$ V, so that we have the 0.7 structure present in two 1D channels in series. The measurement temperature was 1.2 K.

presence of the grounded F2 varies the flow of the electric field lines emitted from F1 and F3, which makes the 2DEG regions underneath F2 less affected by the fringing fields from F1 and F3. All these results demonstrate that for $V_{F1} = \pm 0.22$ V, $V_{F2} = 0$ and $V_{F3} = \pm 0.3$ V, we have two narrower 1D constrictions underneath F1 and F3 in series, present in the ballistic channel defined by SG, as illustrated in Fig. 5. Here we estimate the constriction width underneath F1 (F3), assuming that the lateral (the y component) confining potential in the 1D channel has a form [37]

$$U(y) = U(0) + \frac{1}{2}m^* \omega_y^2 y^2; \quad (1)$$

where $m^* = 0.067 m_e$ and m_e is the electron mass.

From the source-drain biased measurements we know that $\hbar E_{1,2} = 2.434 \text{ meV} = \hbar \omega_y$. The difference between the first 1D subband and the conduction band edge is simply $\frac{1}{2} \hbar \omega_y$ in a simple harmonic oscillator. Thus we calculate ω_y to be $3.698 \times 10^{12} \text{ s}^{-1}$ and $U(0)$ to be 5.78 meV. The 1D channel width can be estimated when the energy of the first 1D subband crosses the Fermi energy in the bulk 2DEG ($E_F = 7 \text{ meV}$). From this we calculate that the constriction width underneath F1 (F3) at the Fermi energy is 43.3 nm. As shown in Fig. 4, we can see that the 0.7 structure is still observed when the two 1D constrictions are in series but occurs at a slightly

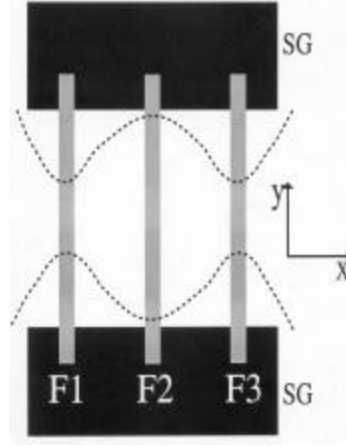


FIG. 5. A schematic diagram showing that applying negative voltages on F1 and F3 creates two narrower 1D constrictions in series. The dotted lines indicate the depletion regions.

less negative V_{SG} . This is to be expected since two gate fingers are being biased rather than one and there is a small degree of cross talk between F1 and F3. The ratio of the reduction of pinch-off voltage to the initial pinch-off voltage is only $0.04/2.65 = 1.5\%$. If the 0.7 structure were a transmission effect, then when we have 0.7 structure present in two 1D channels in series, a shoulder like structure close to $0.7 \text{ } \hbar$ $0.7 = 0.49 (2e^2 = \hbar)$ should have been observed. Instead, the 0.7 structure persists and behaves as if it is like two ballistic resistors in series as first studied by Wharam *et al.* [38] and reproduced here. Thus our experimental results show that the 0.7 structure is *not* a transmission effect through a clean one-dimensional channel at zero in-plane magnetic field.

III. A strongly modulated 1D channel with double barriers: an open quantum dot

Let us turn our attention to the case of a strongly modulated 1D channel with double barriers. We can define a lateral quantum dot by applying voltages on SG, F1 and F3 while keeping F2 grounded to the 2DEG. The data that we report here was obtained from Device C. Trace 1 in Fig. 6 shows the gate characteristics $G(V_{SG})$ for $V_{F1} = \text{ } \mu\text{m} 1.941 \text{ V}$ and $V_{F3} = \text{ } \mu\text{m} 1.776 \text{ V}$ at $T = 50 \text{ mK}$. Periodic and continuous conductance oscillations superimposed on ballistic conductance steps are observed. We ascribe the observed conductance oscillations for $G < 2e^2 = \hbar$ to Coulomb charging effects [39-41]. The observed periodic conductance oscillations for $G > 2e^2 = \hbar$ are unexpected and are one of the main subjects of this paper. Unlike lateral quantum dots whose tunnel barriers are defined by two pairs of split-gates, in our system, the tunnel barriers arise from depletion from overlying finger gates. This causes a large barrier thickness, so that we do not observe well-isolated single electron tunnelling peaks beyond pinch-off in our case. In contrast to the well-quantised conductance plateaux shown in Fig. 1(a), applying voltages to F1 and F3 results in conductance steps that are not as flat or well quantised. With the finger gates grounded to the 2DEG, the channel pinches-off at $V_{SG} = \text{ } \mu\text{m} 1.8 \text{ V}$ compared with $V_{SG} = \text{ } \mu\text{m} 0.7 \text{ V}$ when $V_{F1} = \text{ } \mu\text{m} 1.941 \text{ V}$ and $V_{F3} = \text{ } \mu\text{m} 1.776 \text{ V}$. Thus as voltages are applied to F1 and F3, the lateral

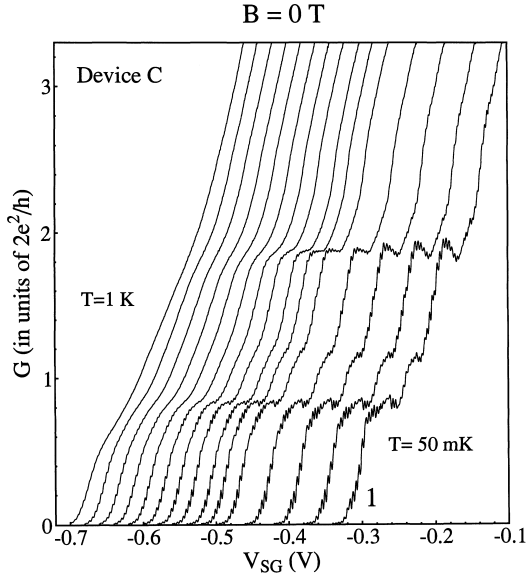


FIG. 6. $G(V_{SG})$ for $V_{F1} = \downarrow 1.941$ V, $V_{F2} = 0$ V, and $V_{F3} = \downarrow 1.776$ V at various temperatures T . From left to right: $T = 1, 0.5, 0.45, 0.41, 0.35, 0.3, 0.26, 0.2, 0.18, 0.17, 0.15, 0.11, 0.09, 0.065$ and 0.05 K. Curves are successively displaced by a horizontal offset of 0.02 V for clarity. The data was obtained from Device C.

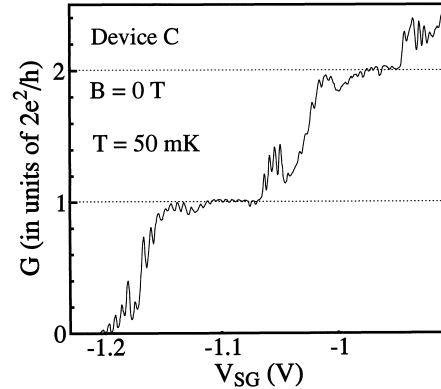


FIG. 7. $G(V_{SG})$ for $V_{F1} = \downarrow 1.1$ V, $V_{F2} = 0$ V, and $V_{F3} = \downarrow 1.0$ V.

confinement weakens and the conductance steps become less pronounced. The conductance steps also deviate from their quantised values. The most likely reason for this effect is due to the introduction of two tunnel barriers which enhances back-scattering in the channel, thereby reducing the transmission probability of 1D channels [37] to be less than 1. However, as shown in Fig. 7, continuous and periodic conductance oscillations are also observed when well-quantised 1D ballistic conductance steps are present. Thus we suggest that the slight deviation from perfect transmission only varies the background conductance in our system and has little effect on the observed continuous and periodic conductance oscillations in V_{SG} shown in both Fig. 6 and Fig. 7.

Previously in a lateral quantum dot [39-41] it has been observed that Coulomb oscillations increase in height and decrease in width as the conductance decreases. This increase in height arises from an accumulation of the electron wavefunction in the dot, giving rise to resonant coherent effects as the dot becomes isolated from the source and drain contacts. From figure 6 we can see that no such increase in height is observed in our system as the conductance is decreased. We believe that the thicker tunnel barriers in our system make it more difficult for the electrons to tunnel out, so that the electron lifetime within the dot becomes so large it exceeds the inelastic scattering time. In such a situation resonant coherent effects decrease with the result that the Coulomb blockade peaks do not increase in height close to pinch-off. We also find that

the peak widths do not decrease as G decreases. Generally for $G > 2e^2/h$, it is expected that the presence of a fully transmitted 1D channel might cause mode mixing between 1D channels in the quantum dot which smears out Coulomb charging effects. However, since our samples are fabricated on an ultra high-quality HEMT, it is likely that there is little 1D mode mixing, so that the level broadening for Coulomb oscillations is similar for both cases when $G < 2e^2/h$ and $2e^2/h < G < 4e^2/h$. Thus as G decreases, the oscillations observed in our system do not appear to decrease in width.

Having defined a lateral quantum dot, we now calculate the dot size and the number of electrons it contains, following the method described in the work by Field and co-workers [42]. For $V_{SG} = 0.5$ V, $V_{F1} = 1.941$ V, and $V_{F3} = 1.776$ V, we observe Aharonov-Bohm (AB) type oscillations as a function of applied perpendicular magnetic field [43] with a period ΦB of 14.7 mT, giving a dot area A of 2.81×10^{13} m². Using the split-gate to change the dot area at a constant magnetic field of 0.8 T, the Aharonov-Bohm period [44, 45] of oscillations ΦV_{SG}^{AB} is measured to be 8.772 mV. Thus $\Phi V_{SG}^{AB}/\Phi A = 1.70 \times 10^{12}$ Vm⁻². Each CB oscillation corresponds to removing an electron from the dot so that the reciprocal of the CB period $\Phi N/\Phi V_{SG}^{CB}$ is 263.3 V⁻¹. From the product of these two terms we obtain the local carrier density in the dot to be 4.47×10^{14} m⁻². Combining this value with the dot area A gives the number of electrons in the dot $N \approx 126$. From the local Fermi energy E_F^{loc} and the number of electrons within the dot, we estimate the 0D confinement energy $E_F^{loc} = N$ to be at most 12.4 meV, comparable to the thermal smearing at 125 mK. The reason for this is due to the large area of our sample. Therefore electron transport through our quantum dot can be described in terms of a classical Coulomb charging picture where the 0D quantum confinement energy is much smaller than the Coulomb charging energy, similar to the case of a metal.

As shown in Fig. 6, for $G < 2e^2/h$, the conductance oscillations persist up to $T = 1$ K. The oscillations for $G > 2e^2/h$ have a strong temperature dependence and become unobservable above $T = 410$ mK. Note that the thermal broadening $k_B T$ at this temperature is still much larger than the estimated 0D quantum confinement energy, excluding an interpretation that conductance oscillations for $G > 2e^2/h$ are due to tunnelling through 0D states in the quantum dot. To determine the total capacitance between the dot and the gates of the sample, we measure the conductance oscillations by varying the voltage on the different gates, while keeping the voltages on the remaining gates fixed. From this we obtain $\Phi V_{F1} = 23.81$ mV, $\Phi V_{F2} = 8.68$ mV, $\Phi V_{F3} = 25.89$ mV, and $\Phi V_{SG} = 3.59$ mV. According to this the total gate-dot capacitance C_g is estimated to be 7.58×10^{17} F. Neglecting the capacitance between the dot and the 2DEG reservoirs, we calculate the Coulomb charging energy e^2/C_g to be 0.211 meV, comparable to the thermal broadening at $T \approx 2$ K, which is consistent with the observation that close to pinch-off Coulomb oscillations persist up to 1 K.

In order to study the unexpected presence of periodic conductance oscillations for $G > 2e^2/h$ in more detail, we have measured their dependence on barrier transparency. Figure 8(a) shows $G(V_{SG})$ as V_{F1} and V_{F3} are simultaneously decreased, thus increasing barrier height (decreasing barrier transparency) at zero magnetic field. Figure 8(b) is a continuation of Fig. 8(a) at even more negative finger gate voltages. We number peaks in $G(V_{SG})$ counted from pinch-off. Note that at pinch-off, we estimate that there are still ≈ 70 electrons within the dot. Consider the sixth single electron tunnelling peak counted from pinch-off. It is evident that as the barrier heights are raised, by making the gate finger voltages more negative, the peak height decreases, and the peak occurs at a less negative V_{SG} , i.e., where the channel is wider. Thus, effectively,

we are keeping the number of electrons within the dot constant while changing the dot shape. We note that the first ten tunnelling peaks counted from pinch-off in Fig. 8(a) gradually disappear as the finger gate voltages are made more negative. This is due to the increasing barrier thickness such that tunnelling conductance becomes immeasurably small [42]. Over the whole measurement range, we can follow up to 48 conductance tunnelling peaks at various V_{F1} (V_{F3}) and are thus able to study their barrier transparency dependence. Note that the observed conductance oscillations for $G > 2e^2/h$ have the *same* period as that of the oscillating features for $G < 2e^2/h$. Most importantly, as shown in Fig. 8(a) and (b), peaks 31-48, where $G > 2e^2/h$ (shown in the uppermost curve), all gradually evolve into conductance oscillations for $G < 2e^2/h$, due to Coulomb charging [39-41] as the barrier heights and thickness increase. This result strongly suggests that the conductance oscillations (for peak 31-48 in the uppermost curve shown in Fig. 8(a)) and the oscillations shown in the lowermost curves (Fig. 8(b)) are of the *same* physical origin—Coulomb charging, compelling experimental evidence for charging effects in the presence of fully transmitted 1D subbands at *zero* magnetic field.

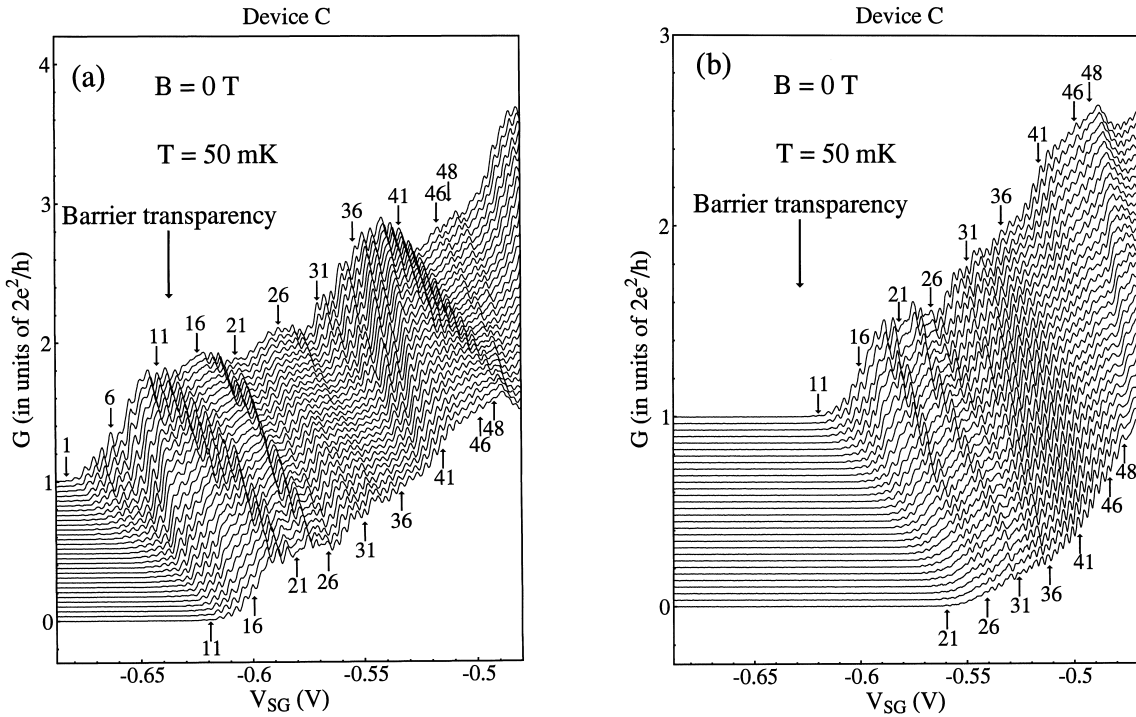


FIG. 8. (a) $G(V_{SG})$ at various voltages applied on F1 and F3 at zero magnetic field. From top to bottom: $V_{F1} = \downarrow 1.907$ V to $\downarrow 1.965$ V in 2 mV steps ($V_{F3} = \downarrow 1.733$ V to $\downarrow 1.805$ V in 2.5 mV steps) (b) Continuation of figure 3(a). From top to bottom: $V_{F1} = \downarrow 1.965$ V to $\downarrow 2.023$ V in 2 mV steps ($V_{F3} = \downarrow 1.805$ V to $\downarrow 1.8775$ V in 2.5 mV steps) Curves are successively offset by $(0.0344)(2e^2/h)$ for clarity. Conductance tunnelling peaks are numbered to serve a guide to the eye for the evolution of oscillating structures in $G(V_{SG})$.

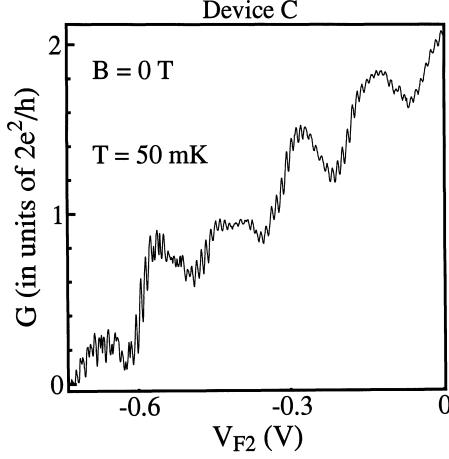


FIG. 9. $G(V_{F2})$ for $V_{F1} = 1.941$ V, $V_{SG} = 0.3$ V, and $V_{F3} = 1.776$ V.

Finally we present clear experimental evidence that coherent resonant transport and Coulomb charging effects co-exist in our system. Figure 9 shows $G(V_{F2})$ for $V_{F1} = 1.941$ V, $V_{SG} = 0.3$ V and $V_{F3} = 1.776$ V when the dot is defined. Periodic and continuous conductance oscillations superimposed on weak resonant features are clearly observed. Decreasing V_{F2} has two effects. First, it depletes the electrons within the open quantum dot, causing successive conductance oscillations due to Coulomb charging effects over the whole measurement range. Second, it also reduces the number of transmitted 1D channels through the dot. The latter effect gives rise to the slowly-varying background – Fabry-Pérot type resonant effects [46] between the entrance and exit to the quantum dot. The maxima (minima) in conductance correspond to constructive (destructive) electron-wave interference effects. This interpretation is further supported by recent theoretical work of Tkachenko and co-workers [47-49]. Thus in order to model our experimental results, the co-existence of coherent transport and Coulomb charging effects must be taken into account.

IV. Conclusions

In conclusion, we have presented low-temperature transport measurements on modulated one-dimensional channels. We have explicitly shown that the “0.7 structure” is an intrinsic property of a clean one-dimensional channel, even when quantised ballistic plateaux are no longer observable for weak lateral confinement. We have also shown that the 0.7 structure present in two 1D channels in series behaves like a single 1D channel which shows the 0.7 structure, demonstrating that the 0.7 structure is not a transmission effect through a ballistic channel at zero in-plane magnetic field.

By strongly modulating the 1D channel with two barriers at either end, periodic and continuous oscillations superimposed upon ballistic conductance steps are observed even when the conductance through the quantum dot is greater than $2e^2/h$. At zero magnetic field, a direct transition of conductance oscillations for $G > 2e^2/h$ to those for $G < 2e^2/h$ due to Coulomb charging effects is observed with decreasing barrier transparencies. The temperature dependence

of the observed oscillating features for $G > 2e^2/h$ excludes an interpretation that they are due to tunnelling through single-particle confinement energy states within the dot. Both results strongly suggest that, at zero magnetic field, charging effects can occur in the presence of a transmitted one-dimensional channel, in contrast to the current experimental and theoretical understanding of Coulomb charging.

V. Acknowledgements

This work was funded by the UK EPSRC. We thank D.G. Baksheyev, C. H. W. Barnes, F. Fang, C. J. B. Ford, J. D. F. Franklin, J. E. F. Frost, S. Gardelis, A. R. Hamilton, M. Kataoka, J. T. Nicholls, S. Shapira, V. I. Talyanskii, K. J. Thomas, O. A. Tkachenko and V. A. Tkachenko for fruitful discussions. C. T. L. acknowledges financial support from the NSC, Taiwan and the Royal Society, UK. M. Y. S. is grateful for support from the ARC. G. H. K. acknowledges financial assistance from the Skillman Fund, Clare College, Cambridge and the Korean MIC.

References

- [1] T. J. Thornton *et al.*, Phys. Rev. Lett. **56**, 1198 (1986).
- [2] D. A. Wharam *et al.*, J. Phys. C **21**, L209 (1988).
- [3] B. J. van Wees *et al.*, Phys. Rev. Lett. **60**, 848 (1988).
- [4] N. K. Patel *et al.*, Phys. Rev. B **44**, R10973 (1991).
- [5] K. J. Thomas *et al.*, Phys. Rev. Lett. **77**, 135 (1996); Phys. Rev. B **58**, 4846 (1998).
- [6] A. Kristensen *et al.*, J. Appl. Phys. **83**, 607 (1998).
- [7] B. E. Kane *et al.*, Appl. Phys. Lett. **72**, 3506 (1998).
- [8] A. Kristensen *et al.*, Physica B **251**, 180 (1998).
- [9] D. Kaufman *et al.*, Phys. Rev. B **59**, R10433 (1999).
- [10] C.-T. Liang *et al.*, Appl. Phys. Lett. **75**, 2975 (1999).
- [11] C.-T. Liang *et al.*, Phys. Rev. B **61**, 9952 (2000).
- [12] A. Kristensen *et al.*, Phys. Rev. B **62**, 10950 (2000).
- [13] K. S. Pyshkin *et al.*, Phys. Rev. B **62**, 15842 (2000).
- [14] D. J. Reilly *et al.*, Phys. Rev. B **63**, R121311 (2001).
- [15] A. Gold and L. Calmels, Philos. Mag. Lett. **74**, 33 (1996).
- [16] L. Calmels and A. Gold, Solid State Commun. **106**, 139 (1998).
- [17] C.-K. Wang and K.-F. Berggren, Phys. Rev. B **54**, R14257 (1996).
- [18] C.-K. Wang and K.-F. Berggren, Phys. Rev. B **57**, 4552 (1998).
- [19] D. Schmeltzer *et al.*, Philos. Mag. B **77**, 1189 (1998).
- [20] H. Bruus, V. V. Cheianov and K. Flensberg, cond-mat/0002338 (2000).
- [21] C. G. Smith *et al.*, J. Phys. C **21**, L893 (1988).
- [22] U. Meirav, M. A. Kastner, and S. J. Wind, Phys. Rev. Lett. **65**, 771 (1990).
- [23] For a review, see H. van Houten, C. W. J. Beenakker, and A. A. M. Staring in *Single Charge Tunnelling*, eds. H. Grabert and M. H. Devoret (Plenum, New York 1992).
- [24] P. L. McEuen *et al.*, Phys. Rev. Lett. **66**, 1926 (1991).
- [25] C. J. B. Ford, Nanostructured Materials **3**, 283 (1993).
- [26] B. Su, V. J. Goldman, and J. E. Cunningham, Science **255**, 313 (1992).
- [27] R. C. Ashoori *et al.*, Phys. Rev. Lett. **68**, 3088 (1992).
- [28] L. W. Molenkamp, K. Flensberg and M. Kemerink, Phys. Rev. Lett. **75**, 4282 (1995).

- [29] C. Pasquier *et al.*, Phys. Rev. Lett. **70**, 69 (1993).
- [30] C.-T. Liang, Ph.D. thesis, Cambridge University (1995).
- [31] C.-T. Liang *et al.*, Phys. Rev. B **55**, 6723 (1997).
- [32] C.-T. Liang *et al.*, Phys. Rev. Lett. **81**, 3507 (1998).
- [33] C.-T. Liang *et al.*, Phys. Rev. B **60**, 10687 (1999).
- [34] C.-T. Liang *et al.*, Appl. Phys. Lett. **76**, 1134 (2000).
- [35] I. Zailer *et al.*, Semicond. Sci. Technol. **11**, 1235 (1996).
- [36] N. K. Patel *et al.*, Phys. Rev. B **44**, 13549 (1991).
- [37] M. Buttiker, Phys. Rev. B **41**, 7906 (1990).
- [38] D. A. Wharam *et al.*, J. Phys. C. **21**, L887 (1988).
- [39] A. A. M. Staring *et al.*, Physica B **175**, 226 (1991).
- [40] L. P. Kouwenhoven *et al.*, Z. Phys. B **85**, 367 (1991).
- [41] J. G. Williamson *et al.*, in *Nanostructures and Mesoscopic Systems*, eds. W. P. Kirk and M. A. Reed, (Academic Press, New York, 1992), p. 225.
- [42] M. Field *et al.*, Phys. Rev. Lett. **70**, 1311 (1993).
- [43] B. J. van Wees Phys. Rev. Lett. **62**, 2523 (1989).
- [44] D. A. Wharam *et al.*, J. Phys. Cond. Matter **1**, 3369 (1989).
- [45] R. J. Brown *et al.*, J. Phys. Cond. Matter **1**, 6291 (1989).
- [46] C. G. Smith *et al.*, J. Phys. Cond. Matter **1**, 6763 (1989).
- [47] O. A. Tkachenko *et al.*, Cond-mat/0003021 (2000).
- [48] O. A. Tkachenko *et al.*, J. Phys. Condens. Matter **13**, 9515 (2001).
- [49] V. A. Tkachenko *et al.*, JETP Lett. **74**, 209 (2001).